





Integrating Geometric Metamodel-Assisted Process Assurance into Topology Optimization of Low-Pressure Die Castings

Tobias Rosnitschek¹  , Maximilian Erber² ,
Christoph Hartmann² , Bettina Alber-Laukant¹ , Wolfram Volk² ,
and Stephan Tremmel¹ 

¹ Engineering Design and CAD, University of Bayreuth, 95643 Bayreuth, Germany
{tobias.rosnitschek,bettina.alber,stephan.tremmel}@uni-bayreuth.de

² Metal Forming and Casting, Technical University of Munich, 85748 Garching, Germany
{maximilian.erber,christoph.hartmann,wolfram.volk}@utg.de

Abstract. Integrating complex process knowledge into structural optimization of casting parts enables design proposals to exploit manufacturing processes' full potential. However, a significant bottleneck for integrating process knowledge is the computational effort necessary for process simulations. In this article, we focused on low-pressure die casting. We used the medial axis transform and the shortest path algorithm to describe geometry-related features that we used as input data for a neural network metamodel, which replaced the casting process simulation. This allowed us to reduce the time for process simulation from multiple hours to a few seconds and, thus, incorporate the metamodel into the topology optimization framework. To reconstruct the geometry, we used an implicit modeling approach in which the modified geometry was built from volume lattices filtered afterward to obtain solid volumes. The approach was tested on two application examples and proved that the metamodel-based results are equivalent to the results obtained using casting process simulations.

Keywords: Topology Optimization · Process Assurance · Medial Axis Transform · Neural Networks · Implicit Modelling

1 Introduction

Two key pillars for developing new products are climate neutrality and energy efficiency. Casting processes have the capability to combine both pillars advantageously by fabricating complex structures at high volumes [1, 2]. Accordingly, we can derive

Tobias Rosnitschek and Maximilian Erber contributed equally

two main objectives, on the one hand lightweight structures that minimize material usage, respectively energy consumption during the product life cycle. On the other hand, efficient and error-free manufacturable geometries, which minimize the scrap-rate. However, the search for a “perfect part” that combines both objectives is difficult. A major bottleneck is the integration of time-consuming process assurance simulation into a topology optimization framework. In this article, we integrate the process assurance via a geometric feature-based artificial neural network metamodel and modify the geometries using implicit modelling.

1.1 Background

Topology optimization is a widely used method for numerical structural optimization with the purpose of identifying the best material distribution in a given design space [3–6]. Nevertheless, optimized design proposals are often non-manufacturable. Therefore, manufacturing constraints are commonly used, for casting processes, these are, among others, minimum length scale, symmetry, extrusion, or parting lines [7–9].

These manufacturing constraints represent a simplification of the unconstrained optimization problem and cannot describe the limits of stable casting processes [10]. Since the major bottleneck for the efficient integration of process assurance is the time-consuming process assurance simulation, the use of computationally cheap metamodels can leverage the quality of casting design proposals significantly.

Such metamodels are often built upon machine learning models, inspired by the idea that in particular artificial neural networks represent universal approximators [11]. Accordingly, machine learning is widely used in manufacturing related topics as energy consumption, wear modelling or tool wear prediction [12–14]. In the context of casting processes, metamodels were applied to predict the results of 2D-casting simulations [15], properties such as hardness based on process parameters [16], or for increasing the product quality by optimizing initial temperature and wall temperature [17].

All the named examples apply machine learning algorithms to optimize process parameters or conditions but are not used within the context of adapting the part’s geometry. Accordingly, for the objective of combining topology optimization with process assurance, well suited machine learning models are not yet identified. The task of searching a well-suited machine learning model for a new problem is difficult, since selecting algorithms and adjacent hyperparameters can be extremely costly. Automated machine learning systemizes the searching or selecting procedure [18, 19]. An efficient method for a neural architecture search system provides the work of Jin et al., where the search space is explored via morphing the neural network architectures guided by a Bayesian optimization algorithm [19]. Automated machine learning approaches do not guarantee to outperform human guided modelling, but they can provide a helpful assistance tool in the modelling process.

1.2 Approach

The objective of this article is to use a geometric feature-based metamodel to replace the casting simulation within a topology optimization process assurance framework, as we show in Fig. 1.

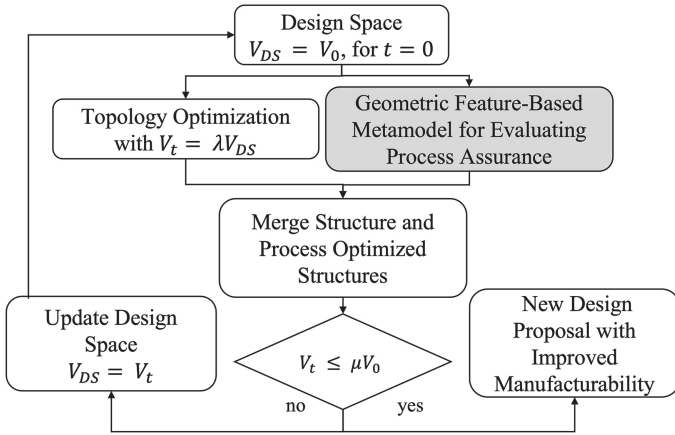


Fig. 1. Metamodel assisted framework for combined topology optimization and process assurance based on the workflow presented in [10]. A topology optimization with an initial Volume V_0 and a target Volume $V_t = \mu V_0$ with volume constraint μ and step length λ is conducted parallel to a casting simulation for process assurance. The latter is replaced by the metamodel (shaded in grey).

In this article, we replace the time-consuming casting simulation by a geometric feature-based metamodel for process assurance. Subsequently, we use implicit modeling to modify the design proposals based on the given evaluation criterion along with the topology optimization results. We apply this approach to a cantilever beam and a traverse link, shown in Fig. 2, and compare the modified design proposals with simulation-based geometry modification.

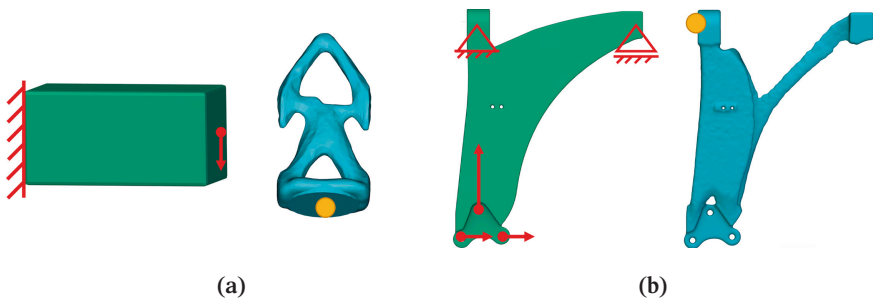


Fig. 2. Overview of the design space (green) and optimized design proposals without integrated process assurance (blue) for the two test examples. (a) Cantilever beam; (b) Traverse link. The load case is sketched in red on the design spaces, while the ingate position is marked orange on the design proposals.

2 Materials and Methods

2.1 Metamodel Architecture

In this article, we used artificial neural networks as metamodels. For preparing the data, building, optimizing and evaluating the metamodel, we used the python libraries numpy [20], seaborn [21], pandas [22, 23], matplotlib [24, 25], scikit-learn [26], scikit-optimize [27], TensorFlow[28, 29], Keras [30, 31] and Auto-Keras [19]. Figure 3 shows the general architecture of the artificial neural network.

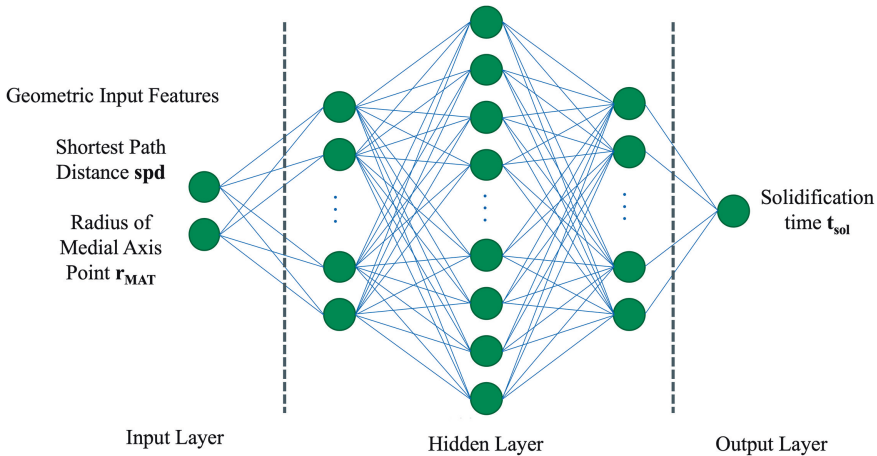


Fig. 3. Architecture of the baseline feed forward multilayer perceptron. Two geometric input features are used to estimate the solidification time in low-pressure die castings.

The baseline model was a dense feed forward multilayer perceptron neural network. We optimized the architecture and the hyperparameters using a two-step automated machine learning approach. The output parameter is the solidification time, which we obtained from previously made casting simulations. As geometric input features, we used shortest path distances, which provide the shortest distance between the ingate and any point in the geometry, and the radii of the medial axis points obtained by the medial axis transform, which represent the part thickness along the solidification path. The calculation of both geometric input features is shortly explained in the following.

Medial Axis Transform. The medial axis transform is a surface skeletonization technique for three dimensional objects, which is calculated from the Voronoi diagram. Every point on the medial axis is associated to an internal ball that touches the part's surface but does not penetrate it [32]. The radii of the balls provide therefore the part thickness for every point on the medial axis. We used the implementation presented in our previous work [32].

Dijkstra's Shortest Path. Dijkstra's shortest Path algorithm begins at a starting node and gradually selects the currently most favorable paths via the nodes on a graph that can be reached next [33]. We used the shortest path to calculate the shortest flow distances between the ingate and all points on the medial axis, thus providing qualitative information how fast a point can possibly be reached by the melt.

Data Preparation. For training and testing the models, we used a dataset containing 220,000 pairs of shortest path distance, radius of medial axis point, and solidification time. The data was split into 200,000 training and 20,000 test data.

Automated Machine Learning. The two-step automated machine learning approach consists of Bayesian optimization supported search for an well suited architecture and a subsequent hyperparameter optimization using the hyperband algorithm [34]. The objective for both optimization tasks was to minimize the mean squared error. During both optimizations, a 5-fold cross-validation was used on the training data. Table 1 shows the selected parameters summarized.

Table 1. Summary of the chosen settings for two-step automated machine learning. The objective function was in both cases the mean squared error (MSE).

	Algorithm	Objective	Iterations
Architecture Search	Bayesian Optimization	MSE	100
Hyperparameter Optimization	Hyperband	MSE	250

2.2 Evaluation of Process Assurance

The process assurance is evaluated using the evaluation criterion developed in our previous work for low-pressure die castings [10]. By assuming a directional solidification in low-pressure die casting, the ratio of the solidification time (t_{sol}) and the shortest path distance (spd) should be descending along the solidification path, which we evaluated using the following equation:

$$QL = \log \left(\frac{t_{sol}}{spd} \right) \quad (1)$$

2.3 Modification of the Design Space

To modify the design spaces, we used the software nTopology (Version 3.35, nTopology Inc., New York, NY, USA) that allows an implicit representation of geometries. Based on the density values of the topology optimization, we first create a volume lattice for activated (high-density, material) and deactivated (low-density, holes) elements, which strut diameters are further adapted by the evaluation criterion point map of QL. We illustrate this procedure in Fig. 4.

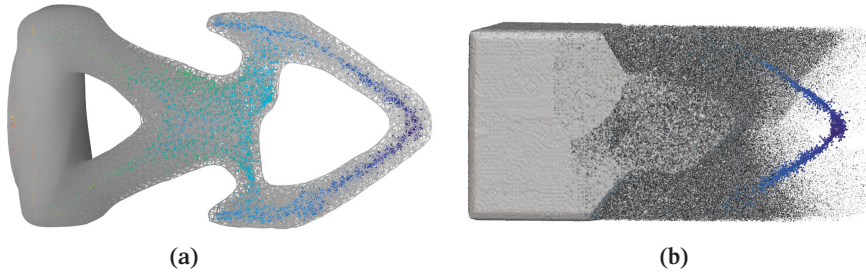


Fig. 4. Volume lattices for (a) activated elements and (b) deactivated elements. The colored point map represents the evaluation criterion's value on each cell of the design proposal.

This procedure allows further the filtering of geometric features according to the lattice density. Subsequently, the activated geometry and the deactivated geometry are filtered, smoothed, and merged, as we show in Fig. 5. The result is a modified design proposal with increased manufacturability.

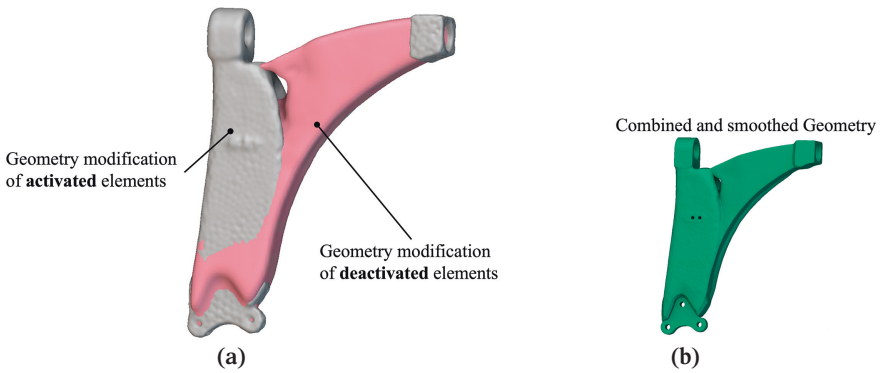


Fig. 5. Illustration of the reconstruction process: (a) The filtered meshes for activated (grey) and deactivated (red) elements are merged. (b) Combined and smoothed geometry which represents the final design proposal.

3 Results and Discussion

3.1 Metamodel Performance

We show the results of the metamodel performance in Fig. 6 by plotting the predicted solidification times ($y_{\text{predicted}}$) against the true – or target – solidification times (y_{target}). For the cantilever the coefficient of determination (R^2) reached 0.79, while the

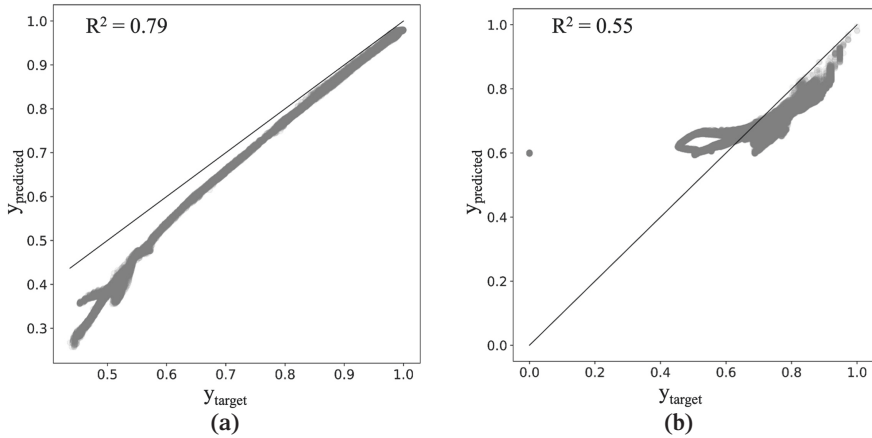


Fig. 6. Results for the metamodel performance for (a) cantilever beam; (b) traverse link.

prediction for the traverse link reached 0.55. This result is plausible due to the cantilever's simpler geometry.

However, since the metamodel's objective is an acceptable estimation rather than a high-fidelity prediction, the achieved results show sufficient accuracy for both test examples.

3.2 Evaluation of Modified Design Proposals

To evaluate the modified design proposals, the QL was first calculated using the predicted solidification times. In the next step the calculated QL modifies the geometries according to the process described in Sect. 2.3. In the following the final metamodel-based design proposals are compared to the simulation-based design proposals. Figure 7 shows that for the cantilever beam the difference volume between metamodel and simulation design proposal is close to zero (Fig. 7b). Accordingly, the presented metamodel-based approach led to equivalent design proposals.

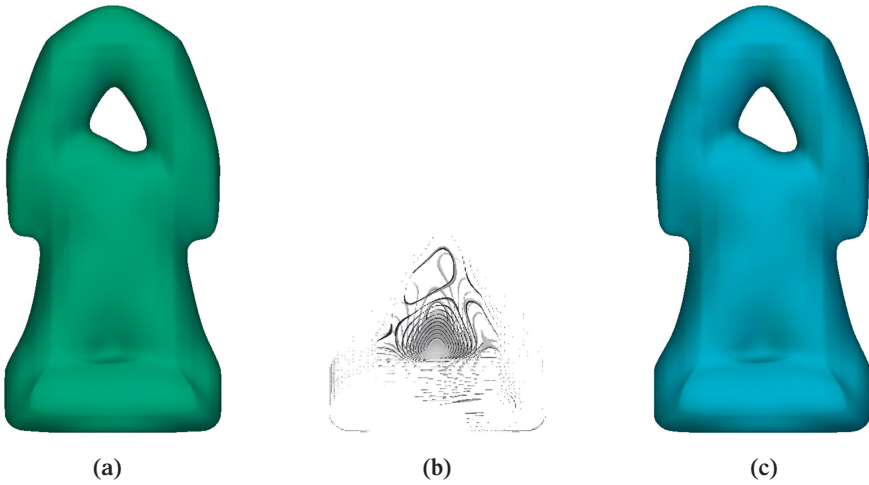


Fig. 7. Comparison of the final cantilever beam design proposals for (a) metamodel-based; (c) simulation-based. (b) represents the difference Volume between both design proposals.

The comparison of the traverse link design proposals shows Fig. 8. In this case deviations between simulated and predicted solidification were significantly greater, which also resulted in deviation of the modified design proposals. In both design proposals, the reconstruction aimed to better connect the box with drill hole on the left side (Fig. 2b) to the rest of the geometry. Interestingly, the metamodel's deviations led to a design proposal, which – geometrically – looks superior the simulation-based proposal.

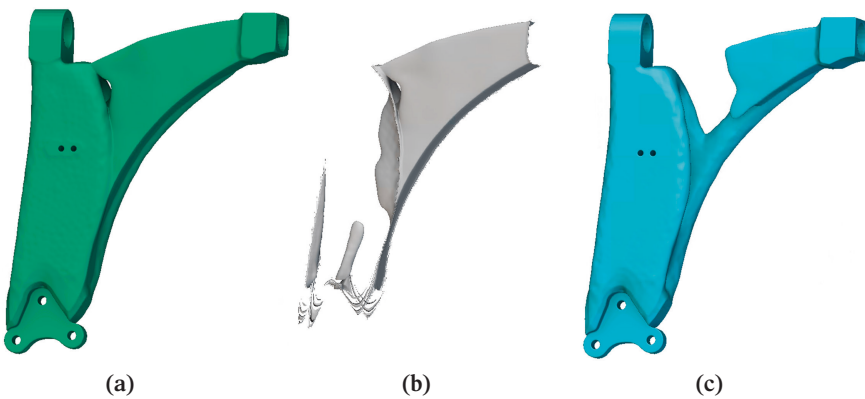


Fig. 8. Comparison of the final traverse link design proposals for (a) metamodel-based; (c) simulation-based. (b) represents the difference Volume between both design proposals.

We attribute this effect to the evaluation criterion calculation on the activated elements and further extrapolation of the values on the deactivated elements. Accordingly, we conclude that also for the traverse link the metamodel resulted in an at least equivalent design proposal, though a smaller coefficient of determination.

4 Summary

In this article, we presented an incorporation of process assurance evaluation into a topology optimization framework, using geometric feature-based metamodel. While building the metamodel, we used a two-stage automated machine learning approach which helped to systematically exploit the parameter space and, thus, identifying a well-suited model architecture and hyperparameters.

The built metamodel reduced the needed time for process assurance evaluation from multiple hours to a few seconds while maintaining a sufficient prediction accuracy. The automated geometry reconstruction further mitigated weak points in the design proposal provided by the isolated topology optimization.

Therefore, our presented approach realizes an efficient incorporation of process assurance into structural optimization and fosters its further dissemination and exploitation of lightweight potentials.

Acknowledgements. The Authors would like to thank the German Research Foundation (DFG) for financial support under grant number 434348474.

References

1. Heilmeier, F., Goller, D., Opritescu, D., Thoma, C., Rieg, F., Volk, W.: Support for Ingate Design by Analysing the Geometry of High Pressure Die Cast Geometries Using Dijkstra's Shortest Path Algorithm. *AMR* 1140, 400–407. (2016). <https://doi.org/10.4028/www.scientific.net/AMR.1140.400>.
2. Franke, T., Fiebig, S., Bartz, R., Vietor, T., Hage, J., vom Hofe, A.: Adaptive topology and shape optimization with integrated casting simulation. In: *EngOpt 2018 Proceedings of the 6th international conference on engineering optimization*, H. C. Rodrigues, J. Herskovits, C. M. Mota Soares, A. L. Araújo, J. M. Guedes, J. O. Folgado, F. Moleiro, and J. F. A. Madeira, Eds. Cham: Springer International Publishing, 2019, 1263–1277. https://doi.org/10.1007/978-3-319-97773-7_109.
3. Rieser, J., Zimmermann, M.: Topology optimization of periodically arranged components using shared design domains. *Struct. Multidiscip. Optim.* **65**(1), 1–22 (2021). <https://doi.org/10.1007/s00158-021-03125-5>
4. Sigmund, O., Maute, K.: Topology optimization approaches. *Struct. Multidiscip. Optim.* **48**(6), 1031–1055 (2013). <https://doi.org/10.1007/s00158-013-0978-6>
5. Harzheim, L., Graf, G.: A review of optimization of cast parts using topology optimization: I - Topology optimization without manufacturing constraints. *Struct. Multidisc. Optim.* **30**(6), 491–497 (2005). <https://doi.org/10.1007/s00158-005-0553-x>

6. Wang, J., Sama, S.R., Manogharan, G.: Re-thinking design methodology for castings: 3D sand-printing and topology optimization. *Int. J. Metalcast.* **13**(1), 2–17 (2018). <https://doi.org/10.1007/s40962-018-0229-0>
7. Harzheim, L., Graf, G.: A review of optimization of cast parts using topology optimization: II-Topology optimization with manufacturing constraints. *Struct Multidisc Optim* **31**(5), 388–399 (2006). <https://doi.org/10.1007/s00158-005-0554-9>
8. Vatanabe, S.L., Lippi, T.N., de Lima, C.R., Paulino, G.H., Silva, E.C.N.: Topology optimization with manufacturing constraints: A unified projection-based approach. *Adv. Eng. Softw.* **100**, 97–112 (2016). <https://doi.org/10.1016/j.advengsoft.2016.07.002>
9. Wang, Y., Kang, Z.: Structural shape and topology optimization of cast parts using level set method: Structural shape and topology optimization of cast parts using level set method. *Int. J. Numer. Meth. Engng* **111**(13), 1252–1273 (2017). <https://doi.org/10.1002/nme.5503>
10. Rosnitschek, T., Erber, M., Hartmann, C., Volk, W., Rieg, F., Tremmel, S.: Combining structural optimization and process assurance in implicit modelling for casting parts. *Materials* **14**(13), 3715 (2021). <https://doi.org/10.3390/ma14133715>
11. Hornik, K., Stinchcombe, M., White, H.: Multilayer feedforward networks are universal approximators. *Neural Netw.* **2**(5), 359–366 (1989). [https://doi.org/10.1016/0893-6080\(89\)90020-8](https://doi.org/10.1016/0893-6080(89)90020-8)
12. Weigold, M., Ranzau, H., Schaumann, S., Kohne, T., Panten, N., Abele, E.: Method for the application of deep reinforcement learning for optimised control of industrial energy supply systems by the example of a central cooling system. *CIRP Ann.* **70**(1), 17–20 (2021). <https://doi.org/10.1016/j.cirp.2021.03.021>
13. Nakai, M.E., Aguiar, P.R., Guillard, H., Bianchi, E.C., Spatti, D.H., D’Addona, D.M.: Evaluation of neural models applied to the estimation of tool wear in the grinding of advanced ceramics. *Expert Syst. Appl.* **42**(20), 7026–7035 (2015). <https://doi.org/10.1016/j.eswa.2015.05.008>
14. Caggiano, A., Nele, L.: Fraunhofer Joint Laboratory of Excellence on Advanced Production Technology (Fh-J_LEAPT UniNaples) P.le Tecchio 80, Naples 80125, Italy, Department of Industrial Engineering, University of Naples Federico II, Naples, Italy, and Department of Chemical, Materials and Industrial Production Engineering, University of Naples Federico II, Naples, Italy, “Artificial Neural Networks for Tool Wear Prediction Based on Sensor Fusion Monitoring of CFRP/CFRP Stack Drilling,”. *IJAT* **12**(3), 275–281 (2018). <https://doi.org/10.20965/ijat.2018.p0275>
15. Krimpenis, A., Benardos, P.G., Vosniakos, G.-C., Koukouvtiki, A.: Simulation-based selection of optimum pressure die-casting process parameters using neural nets and genetic algorithms. *Int J Adv Manuf Technol* **27**(5–6), 509–517 (2006). <https://doi.org/10.1007/s00170-004-2218-0>
16. Kittur, J.K., Manjunath Patel, G.C., Parappagoudar, M.B.: Modeling of pressure die casting process: An artificial intelligence approach. *Int. J. Metalcast.* **10**(1), 70–87 (2015). <https://doi.org/10.1007/s40962-015-0001-7>
17. Shahane, S., Aluru, N., Ferreira, P., Kapoor, S.G., Vanka, S.P.: Optimization of solidification in die casting using numerical simulations and machine learning. *J. Manuf. Process.* **51**, 130–141 (2020). <https://doi.org/10.1016/j.jmapro.2020.01.016>
18. Yao, Q. et al.: Taking Human out of Learning Applications: A Survey on Automated Machine Learning. [arXiv:1810.13306](https://arxiv.org/abs/1810.13306) [cs, stat], (2019) Accessed 5 Feb 2022. <http://arxiv.org/abs/1810.13306>
19. Jin, H., Song, Q., Hu, X.: Auto-Keras: An efficient neural architecture search system. In: Proceedings of the 25th ACM SIGKDD international conference on knowledge discovery & data mining, Anchorage AK USA, 1946–1956, July 2019. <https://doi.org/10.1145/3292500.3330648>

20. Harris, C.R., et al.: Array programming with NumPy. *Nature* **585**(7825), 357–362 (2020). <https://doi.org/10.1038/s41586-020-2649-2>
21. Waskom, M.: seaborn: statistical data visualization. *JOSS* **6**(60), 3021 (2021). <https://doi.org/10.21105/joss.03021>
22. Reback, J. et al.: pandas-dev/pandas: Pandas 1.0.3. Zenodo (2020). <https://doi.org/10.5281/ZENODO.3715232>
23. McKinney, W.: Data Structures for Statistical Computing in Python. Paper presented at the Python in science conference, Austin, Texas, 56–61 (2010). <https://doi.org/10.25080/Majora-92bf1922-00a>
24. Caswell, T.A. et al.: matplotlib/matplotlib: REL: v3.5.1. Zenodo (2021). <https://doi.org/10.5281/ZENODO.5773480>
25. Hunter, J.D.: Matplotlib: A 2D graphics environment. *Comput. Sci. Eng.* **9**(3), 90–95 (2007). <https://doi.org/10.1109/MCSE.2007.55>
26. Pedregosa, F., et al.: Scikit-learn: Machine learning in python. *JMLR* **12**, 2825–2830 (2011)
27. Head, T. et al.: Scikit-Optimize/Scikit-Optimize: V0.5.2. Zenodo (2018). <https://doi.org/10.5281/ZENODO.1207017>
28. TensorFlow Developers: TensorFlow. Zenodo (2021). <https://doi.org/10.5281/ZENODO.5799851>
29. Abadi, M. et al.: TensorFlow: Large-scale machine learning on heterogeneous systems. (2015). <https://www.tensorflow.org/>
30. Chollet, F., et al.: Keras. (2015). <https://keras.io>
31. O'Malley, T. et al.: KerasTuner. (2019). <https://github.com/keras-team/keras-tuner>
32. Erber, M., Rosnitschek, T., Hartmann, C., Alber-Laukant, B., Tremmel, S., Volk, W.: Geometry-based assurance of directional solidification for complex topology-optimized castings using the medial axis transform. *Computer-Aided Design* 103394 (2022). <https://doi.org/10.1016/j.cad.2022.103394>
33. Dijkstra, E.W.: A note on two problems in connexion with graphs. *Numer. Math.* **1**(1), 269–271 (1959). <https://doi.org/10.1007/BF01386390>
34. Li, L., Jamieson, K., DeSalvo, G., Rostamizadeh, A., Talwalkar, A.: Hyperband: A novel bandit-based approach to hyperparameter optimization. 52